

Using Lagrangian Coherent Structures to Investigate Tidal Transport Barriers in Moreton Bay, Queensland

Anusmriti Ghosh¹, K. Suara¹, Y. Yu², H. Zhang² and R. J. Brown¹

¹Environmental Fluid Mechanics Research Group
Queensland University of Technology, Queensland 4000, Australia

²School of Engineering and Built Environment
Griffith University, Queensland 4222, Australia

Abstract

Horizontal chaotic dispersion plays an important role in the distribution and fate of pollutants in coastal waters. Particle dispersion within coastal areas is governed by the combination of local weather events and the interaction of the flow field with local morphological structures, at small and large time scales. The present study investigates the horizontal dispersion and barriers to material transport in a tidal dominated estuary (Moreton Bay) using a combination of a hydrodynamic model and the identification of Lagrangian Coherent Structures (LCS) which acts as transport barriers. In this study, Finite-Time Lyapunov Exponent (FTLE) method has been applied to investigate how the material gets close to the LCS and also to identify the characteristics of the LCS for spring and neap tides.

Introduction

Horizontal chaotic dispersion plays an important role in the distribution and fate of pollutants in coastal waters. Particle dispersion within coastal areas is governed by the combination of local weather events and the interaction of the flow field with local morphological structures, at small and large time scales [13]. The superposition of these processes occurring at multiple timescales has been hypothesised to lead to the chaotic nature of particle transport in coastal systems [13]. Within these chaotic patterns are Lagrangian Coherent Structures (LCS) which serve as distinctive barriers which form the pathway for mixing and dispersion of scalar product within the system. Unveiling these structures has applications in location-time management of waste disposal, management of discharge of accidental pollutants, and search and rescue operations, etc.

LCS are the locally the strongest repelling or attracting material lines, and represent the cores of Lagrangian patterns that cannot be crossed by an ideal tracer [6]. While it might be difficult to predict the pathway of a single particle in a chaotic flow condition, identification of material lines which act as barriers of attraction and repulsion for clusters of particles can be helpful in the prediction of areas of accumulation of pollutants. Significant work has been done in the development of the fundamental approaches for uncovering LCS [5]. Application of LCS to velocity fields from hydrodynamic model output of coastal waters is still an on-going area of development. Furthermore, coastal regions are of great ecological and economic interest, therefore intensified investigation of transport processes is necessary. Thus the work investigates the transport barriers in a coastal water, Moreton Bay.

Materials and Method

Field description

Moreton Bay is a semi-enclosed subtropical embayment high in morphologic, ecological and economic significance to

southeast Queensland [4]. The system lies between 27° and 28° south latitude, spans approximately 110 km north to south, and has its major opening to the ocean of approximately 15 km on the northern side (Figure 1). The system holds the discharge from many smaller rivers and estuaries and thus prone to strong changes in physiochemical properties due to anthropogenic activities and storm discharges. It also serves as a natural protection for a section of Australia's east coast from direct wave action. In recent years an increasing number of severe flood events resulted in large sediment transport in the bay. The sub-tropical climate of Moreton Bay is characterised by high rainfall during summer months that can lead to large runoff events and occasional floods, while the base-flow is minimal during the winter dry season [4]. For most of the time, Moreton Bay is characterised as a modified wave-dominated estuary with M2 semi-diurnal tides with a range of 1-2 m [1]. However, the large catchment inflow from the Brisbane and Logan-Albert Rivers, with a catchment area >1,000 km² can exert significant influence on the sediment and water quality of the system [3, 4]. Here we focus on the transport behaviour for a baseline condition. A hydrodynamic model was set up for the period between July 23 and August 6, 2013 (Figure 3) covering the spring and neap tidal types. This period was chosen to overlap the period where field observation with drifters was available for model validation [15].

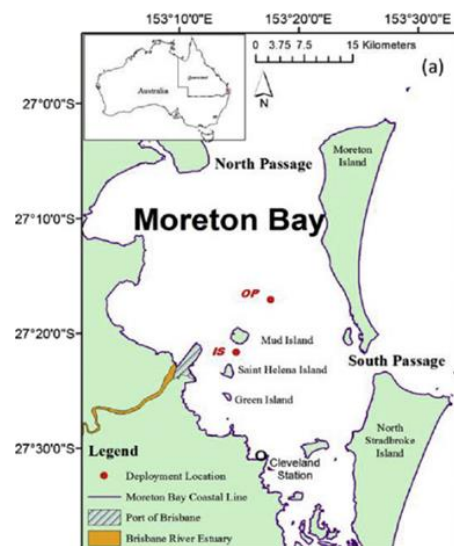


Figure 1. Map of the Moreton Bay shoreline [15].

Model Description

A 3D hydrodynamic MIKE3 DHI was applied in this study. Numerical simulations were conducted with unstructured triangular meshes, a free surface, and 3D incompressible Reynolds-averaged Navier-Stokes equations [2]. Based on the

raw bathymetry data provided by the Griffith Centre for Coastal Management on behalf of Gold Coast City Council, the horizontal domain was presented as a network of flexible unstructured triangular grids, consisting of 13,918 elements (Figure 2). A fine (<100 m) grid resolution was used near the river mouth and near the coastal region, while a relatively coarser grid resolution (ranging from 100 to 500 m) was applied for the far-field areas (Figure 2). In the vertical domain, the variable sigma co-ordinates formulated by [12] were applied, with 10 vertical layers in each water column.

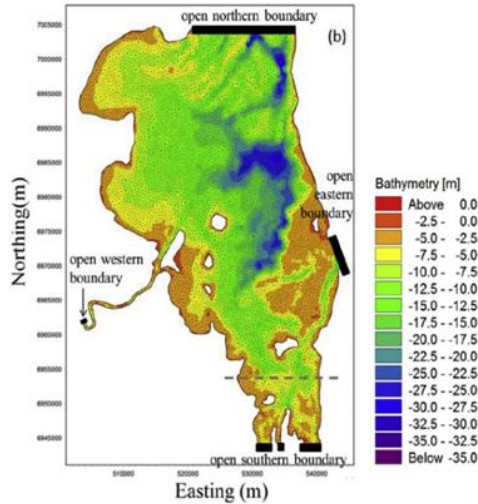


Figure 2. The mesh structure and bathymetry of Moreton Bay [15].

Hourly river discharge data derived from field observations by the Department of Environment and Resource Management, Queensland, Australia, were used at the west boundary for the boundary condition. Tidal elevations at 10-minute intervals provided by Maritime Safety Queensland, Australia, served as open boundary conditions at the northern, eastern and southern boundaries. One-minute interval wind data sourced from the Australian Bureau of Meteorology at a chosen site (153.24 °E, 27.26 °S) was used as model input across the model domain. Figure 3 shows the water level time series from the Brisbane tidal gauge for the period under consideration. A semi-diurnal tidal cycle chosen as a function of time is conducted to account for flow reversal and an effect of residual eddies.

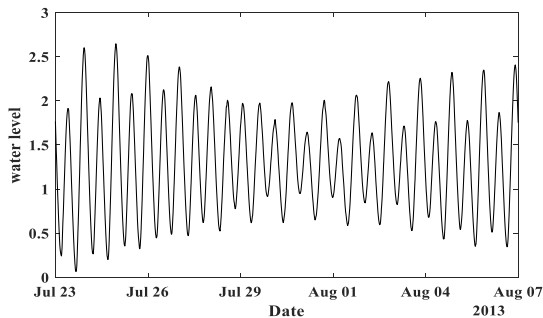


Figure 3. Time series of water level from July 23 to August 6, 2013.

The hydrodynamic model was calibrated and verified using field observed data as detailed in [15]. The model generally produced accurate results for water level, drifter trajectories, water surface temperature and salinity, and vertical temperature and salinity profiles. The RMSE was 0.07 m for water level. The NRMSE of drifter trajectories in longitudinal and lateral directions was 1.26% and 7.45%, respectively. The RMSE of the simulated surface water temperature and salinity during the trip were 0.9° C and 0.23 psu. Further, the vertical distributions of temperature and salinity had RMSEs of 0.8°C and 0.21 psu.

In order to provide discrete velocity input for the LCS analysis, model velocity outputs were stored every 3 min.

Data analysis

The present study investigates the horizontal dispersion and barriers to material transport in a tidal dominated estuary (Moreton Bay) using a combination of hydrodynamic model and identification of LCS. Three major entrances (Figure 1) provide oceanic exchange through tidal flushing of Moreton Bay, with the majority of exchange occurring through the ≈15.5 km wide North Passage and the narrower ≈ 3.7 km wide South Passage [4]. The paper discusses the identification of the material barrier in the tidal embayment for different types of tide using the FTLE method.

To detect the LCS, different types of diagnostic and analytical approaches have been proposed over the past two decades. Based on the ranking of these approaches, FTLE (Finite-Time Lyapunov Exponent) and FSLE (Finite-size Lyapunov Exponent) are more reliable to detect LCS. Therefore, FTLE has been chosen in this work to analyse the material barrier in terms of tidal types. In order to extract LCS, the FTLE fields are computed from the discrete three-minute interval velocity data set of the hydrodynamic model. The FTLE were computed by advecting a grid of artificial tracers for a finite time t using a fourth order Runge–Kutta scheme. The FTLE fields $\Delta(\vec{x}, t, \tau)$ are computed as:

$$\Delta(\vec{x}, t, \tau) = \frac{1}{\tau} \ln \sqrt{\lambda_{max}(\Delta(\vec{x}, t, \tau))} \quad (1)$$

where τ is the advection time and λ_{max} is the largest eigenvalue of the Cauchy-Green deformation tensor $\Delta(\vec{x}, t, \tau)$ [8, 10]. The integration can be performed in the forward or backward direction to unveil the $(\Delta^+(\vec{x}, t, \tau))$ representing the repelling (divergent and unstable) or $(\Delta^-(\vec{x}, t, \tau))$ representing the attracting (convergent and unstable) material lines, respectively. Opposing the forward FTLE field, the backward FTLE fields are those obtained where the tracer field is released at time t and advected with the negative velocity field until time $t + \tau$. The FTLE fields were obtained using the open source FTLE computing code FlowVC [9].

Selection of FTLE resolution and the Integration times

Sensitivity analysis was carried out from which 10 m x 10 m resolution was chosen to calculate the FTLE fields. Studies have shown that the FTLE field and interpretation are sensitive to the maximum integration time. Meaningful FTLE can be obtained using values of τ selected carefully according to two criteria. The τ represents the time scale of the Lagrangian processes that will be mapped in the FTLE fields, therefore a prior knowledge of the time scales of processes is important. If a certain Lagrangian structure with a typical time scale τ_L should be sampled, a much shorter integration time impedes the tracers to explore the whole structure by shortening the trajectories' length; whereas for a much longer advection time, tracers explore many different parts of the flow, so their integrated history becomes similar and the spatial FTLE field becomes more uniform. The advection time τ is analysed in terms of the probability distribution functions (PDF) $p(\Delta^+(\tau))$ of the magnitude of FTLE fields (Figure 4). The PDF of combined FTLE values in Figure 4 is investigated by the choice of τ as a multiple time of the tidal period. Similar to previous studies, as τ increased, the FTLE converged to an asymptotic form of a delta function, which denotes a uniform FTLE field without any spatial information [7]. The loss of

spatial information at large time scale is an indication of a smoother FTLE field with increasing τ . The PDF are shown in vertical log scale to unveil the information carried by the tail of the PDF. For small advection times, the PDF is dominated by the distribution of the local instantaneous strain, thus limiting the scale of structure that could be unveiled. Other than this insight, the evolution of the pdf did not show a preference for selecting the advection time.

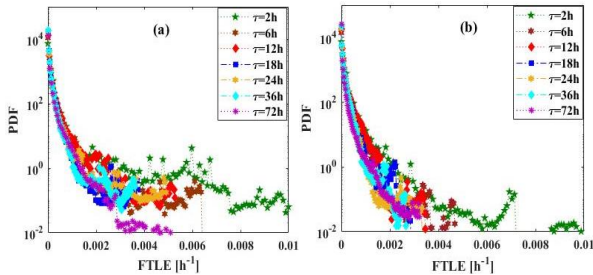


Figure 4. Sensitivity analysis for (a) forward and (b) backward FTLE.

Note that following [11], FTLE are only calculated up the point the tracer reached the boundaries. Previous work has shown that dispersion in Moreton Bay depends strongly on the tidal cycles. Thus, a meaningful way of selecting τ is obtained by considering the average residence time within the domain of interest. The system was strongly tidal dependent within the study period, and for this preliminary analysis, we focused on the material lines around the major inlet. We chose $\tau = 72$ hours for the FTLE. This corresponds to this closest multiple of semi-diurnal tide around the average residence time of 15 km x 15 km area around the northern inlet.

Results and discussions

Presentation

The performance of the mesh structure in the simulation depends on the computation time, flow magnitude, and integration time, and therefore a higher-resolution mesh is required to investigate the more accurate barrier of the LCS. The resolution of the FTLE fields is significantly higher than the velocity fields from the model. From the mesh resolution result, 10m x 10m resolution has been chosen for the total domain to calculate the FTLE field due to computational time (Figure 5). The mean resolution of bathymetry applied in [14] was approximately 500m x 500 m. In order to obtain the meaningful combined FTLE fields, integration time (τ) have been chosen as 72h for this total domain analysis. Velocity is calculated for every 3 minutes, which is 0.05 m/s. High values of the positive and negative time FTLE indicate regions of high particle separation and attraction, which is the stable and unstable manifold coinciding with the location in Figure 5. In forward time, particles on either side of a repelling LCS exponentially diverge away from each other. Similarly, in backward time, particles on either side of an attracting LCS exponentially diverge away from each other. The forward and backward FTLE are shown by positive and negative contours in Figure 5. The marked area has been chosen from Figure 5, for the spring and neap tide analysis (Figure 6 and Figure7) to observe the closer view of the material barrier.

Effect of tidal phase and type on material barriers

Tidal fluctuations play an important role in the natural world and can have a marked effect on maritime-related activities. Tidal waves are commonly categorised as spring and neap tide. A comparison of combined FTLE fields for the spring and neap tide with corresponding water level, at the specific location (set

as northing (6,980,000 m to 7,004,100 m) and easting (520,000 m to 537,000 m)) from the total domain of Moreton Bay, which is marked in Figure 5 are displayed in Figures 6 and 7.

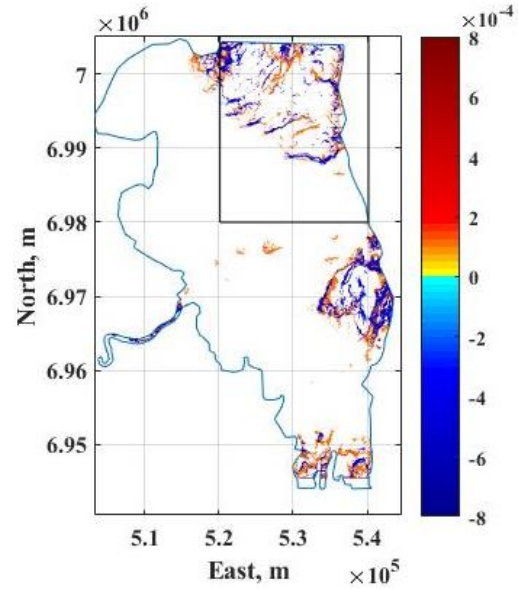


Figure 5. FTLE ($\tau=72h$) analysis for the total domain of Moreton Bay.

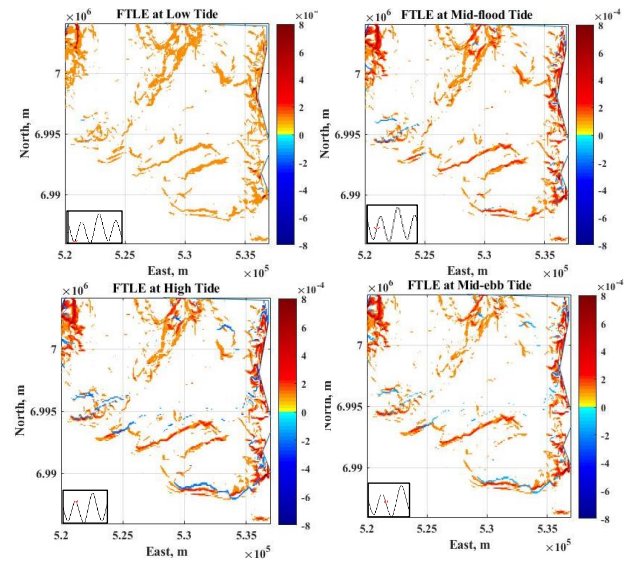


Figure 6. FTLE ($\tau=72h$) analysis for the spring tide of Moreton Bay.

To develop an understanding of the complex internal tidal phenomena in spring tide, we chose multiple of semi-diurnal tide period for the integration time. After comparing the mesh performance, 10m x 10m mesh resolution was chosen to investigate the more accurate hydrodynamic model results. The FTLE is calculated for every 3 hours up to 12 hours from the starting period of the spring tide. Integration time (τ) have been chosen as 72h for this spring and neap tide for the both forward and backward FTLE fields. Figures 6 and 7 show the variation of the transport barriers as a function of the initial tidal phase, from the low tide to the mid-flood tide. The strength of the LCS are time dependent and oscillate with the cycle of the tide as shown in Figure 6. Four different phases of tide have been selected, which are low tide, mid-flood tide, high tide and mid-ebb tide, to differentiate the attracting and repelling material barrier for the spring and neap tides (Figures 6 and

Figure 7). High tides feature most pronounced structures of the material barrier compared to the other phase of spring tide.

The combined FTLE field and corresponding water level have been shown in Figure 7 for neap tide as a function of the tidal phase starting from the low tide to the mid-flood tide. From Figure 7, the accumulations of material barriers in the neap tide are mostly seen in the north-east and north-west areas, however, the material structures in the south-west area were insignificant. This was likely associated with the lower tidal velocity amplitude characterised of the neap tide within the system. It is worth noting gradual formation of vortical structures, near the entrance, which are core for transport of material in the system during low flow. The impacts of tidal fluctuations have larger contribution for transport contamination. However, in the neap tide analysis, a vortex type of LCS means that nested and closed material surfaces have been captured which is really important for this Moreton Bay analysis. The preliminary analysis provided here showed that similar to the spring tidal pattern, the strength of the material barrier changed with the tidal phase while the structures were generally persistent independent of the tidal phase. This suggests that the transport of material within the channel for the baseline condition studied here are connected with local dynamics such as the bathymetry and the islands in Moreton Bay.

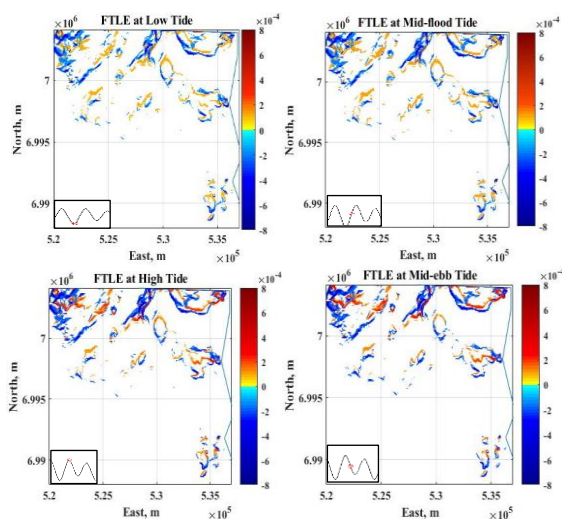


Figure 7. FTLE ($\tau=72h$) analysis for the neap tide of Moreton Bay.

Conclusions

The analysis of tidal flow through FTLE methods demonstrates the importance of LCS in the coastal model. The preliminary analysis provided here showed that similar to the spring tidal pattern, the strength of the material barrier changed with the tidal phase while the structures were generally persistent independent of the tidal phase. This suggests that the transport of material within the channel for the baseline condition studied here are connected with local dynamics such as the bathymetry and the islands in Moreton Bay. This knowledge is important for timing of discharge of effluent from surrounding current and future water treatment including desalination facilities.

Acknowledgments

The project is supported through the Australian Research Council Linkage grant LP150101172.

References

[1] Dennison, W.C.&E.G. Abal, *Moreton Bay study: a scientific basis for the healthy waterways campaign*. 1999:

South East Qld Regional Water Quality Management Strategy Team.

- [2] DHI Water and Environment, *MIKE 21 & MIKE 3 FLOW MODEL FM*. Hydrodynamic and transport module scientific documentation. 2014: DHI.
- [3] Digby, M., P. Saenger, M.B. Whelan, D. McConchie, B. Eyre, N. Holmes,&D. Bucher, *A physical classification of Australian estuaries*. 1999.
- [4] Gibbes, B., A. Grinham, D. Neil, A. Olds, P. Maxwell, R. Connolly, T. Weber, N. Udy,&J. Udy, *Moreton Bay and its estuaries: a sub-tropical system under pressure from rapid population growth*, in *Estuaries of Australia in 2050 and beyond*. 2014, Springer. p. 203-222.
- [5] Hadjighasem, A., M. Farazmand, D. Blazeovski, G. Froyland,&G. Haller, *A critical comparison of Lagrangian methods for coherent structure detection*. *Chaos: An Interdisciplinary Journal of Nonlinear Science*, 2017. **27**(5): p. 053104.
- [6] Haller, G., *Lagrangian Coherent Structures*. *Annual Review of Fluid Mechanics*, 2015. **47**(1): p. 137-162.
- [7] Huhn, F., A. von Kameke, S. Allen-Perkins, P. Montero, A. Venancio,&V. Pérez-Muñuzuri, *Horizontal Lagrangian transport in a tidal-driven estuary—Transport barriers attached to prominent coastal boundaries*. *Continental Shelf Research*, 2012. **39-40**: p. 1-13.
- [8] Mancho, A.M., D. Small,&S. Wiggins, *A tutorial on dynamical systems concepts applied to Lagrangian transport in oceanic flows defined as finite time data sets: Theoretical and computational issues*. *Physics Reports*, 2006. **437**(3-4): p. 55-124.
- [9] Shadden, S., *FlowVC (Version 1)[Computer software]*. Retrieved from <http://shaddenlab.berkeley.edu/software/>. 2010
- [10] Shadden, S.C., F. Lekien,&J.E. Marsden, *Definition and properties of Lagrangian coherent structures from finite-time Lyapunov exponents in two-dimensional aperiodic flows*. *Physica D: Nonlinear Phenomena*, 2005. **212**(3-4): p. 271-304.
- [11] Shadden, S.C., F. Lekien, J.D. Paduan, F.P. Chavez,&J.E. Marsden, *The correlation between surface drifters and coherent structures based on high-frequency radar data in Monterey Bay*. *Deep Sea Research Part II: Topical Studies in Oceanography*, 2009. **56**(3): p. 161-172.
- [12] Song, Y.,&D. Haidvogel, *A semi-implicit ocean circulation model using a generalized topography-following coordinate system*. *Journal of Computational Physics*, 1994. **115**(1): p. 228-244.
- [13] Suara, K., H. Chanson, M. Borgas,&R.J. Brown, *Relative dispersion of clustered drifters in a small micro-tidal estuary*. *Estuarine, Coastal and Shelf Science*, 2017. **194**: p. 1-15.
- [14] Yu, Y., H. Zhang,&C. Lemckert, *Numerical analysis on the Brisbane River plume in Moreton Bay due to Queensland floods 2010–2011*. *Environmental Fluid Mechanics*, 2014. **14**(1): p. 1-24.
- [15] Yu, Y., H. Zhang, D. Spencer, R.J. Dunn,&C. Lemckert, *An investigation of dispersion characteristics in shallow coastal waters*. *Estuarine, Coastal and Shelf Science*, 2016. **180**: p. 21-32.